nature sustainability

Article

https://doi.org/10.1038/s41893-022-01056-7

Afforesting arid land with renewable electricity and desalination to mitigate climate change

Received: 23 June 2022

Accepted: 14 December 2022

Published online: 6 February 2023

Check for updates

Upeksha Caldera & Christian Breyer

Afforestation is one of the most practised carbon dioxide removal methods but is constrained by the availability of suitable land and sufficient water resources. In this research, existing concepts of low-cost renewable electricity (RE) and seawater desalination are built upon to identify the global CO_2 sequestration potential if RE-powered desalination plants were used to irrigate forests on arid land over the period 2030–2100. Results indicate a cumulative CO_2 sequestration potential of 730 $GtCO_2$ during the period. Global average cost is estimated to be €457 per tCO_2 in 2030 but decrease to €100 per tCO_2 by 2100, driven by the decreasing cost of RE and increasing CO_2 sequestration rates of the forests. Regions closer to the coast with abundant solar resources and cooler climate experience the least costs, with costs as low as €50 per tCO_2 by 2070. The results suggest a key role for afforestation projects irrigated with RE-based desalination within the climate change mitigation portfolio, which is currently based on bioenergy carbon capture and storage, and direct air carbon capture and storage plants.

Carbon dioxide removal (CDR) methods have been shown to play varying roles in pathways that limit global warming to 1.5 °C, depending on the rate and depth of reduction of greenhouse gases[1]. The range of CO_2 removal is expected to be between 150 and 1,180 $GtCO_2$ by the end of the century[2]. Out of the CDR methods explored in Integrated Assessment Models (IAMs), one of the most practised CDR methods today is afforestation[1,3,4]. The Food and Agricultural Organisation (FAO) defines afforestation to be the deliberate conversion of non-forested land to forests[5]. Carbon sequestration potentials through global afforestation have been estimated to be up to 1.5 $GtCO_2\,yr^{-1}$ in 2050 at US$50 per tCO_2 (€44 per tCO_2 at an exchange rate of US$1.13 per €), with higher potentials of up to 4.9 $GtCO_2\,yr^{-1}$ at US$200 per tCO_2 (€176 per tCO_2)[4]. The annual CO_2 emissions from the global energy sectors in 2021 are estimated to be 36.3 $GtCO_2$, the highest levels recorded despite the drop in emissions in 2020 due to the Covid-19 pandemic[6,7]. Meanwhile, greenhouse gases with higher global warming potential, such as CH_4 and N_2O, continue to rise[8]. To keep CO_2 emissions at the recommended safer limit of 350 ppm or global temperature rise to about 1°C above the pre-industrial level, it is estimated that the removal of between 561 and 5,976 $GtCO_2$ would be necessary depending on the rate at which emissions are curtailed from 2020 onwards[9].

Afforestation, particularly for economic gain, is considered on productive land without using irrigation systems. This results in competition with agriculture and grazing land[4,10]. Despite low afforestation/reforestation (AR) costs of about US$17–30 per tCO_2 (€15–26 per tCO_2) in 2100 with a mean of US$24 per tCO_2 (€21 per tCO_2), AR has some of the higher land and water requirements of all CDR technologies examined in the study[3]. Thus, it is expected that afforestation will compete with agricultural policies and contribute to increase in food prices[4]. In addition, the growth, survival and productivity of trees are intrinsically dependent on reliable water supply as observed in the mortality of trees in afforestation projects in China and Turkey[11,12]. The water and suitable land constraints have limited the role that afforestation can play in the pathways towards limiting global temperature rise to 1.5 °C.

Seawater reverse osmosis (SWRO) desalination is increasingly seen as a reliable and cost-effective solution to alleviate water scarcity exacerbated by climate change[13]. As the cost of renewables drastically decline and freshwater resources become scarce, renewable electricity

LUT University, Lappeenranta, Finland. e-mail: upeksha.caldera@lut.fi; christian.breyer@lut.fi

(RE)-based SWRO has become an attractive water supply option[13–15]. With increasing water stress (WS) and natural ecosystems being cut down at faster rates to make way for agriculture[16], the goal of this study is to analyse the potential of afforestation if low-cost RE-based SWRO desalination is made available to restore forests on arid or semi-arid lands. Afforestation is generally considered in terms of commercial tree plantations where the trees are cut down after a period of 10–20 yr, releasing the sequestered carbon back into the atmosphere[17]. In this study, the concept of forests that are allowed to grow on arid lands without human disturbance for several decades is explored. A combination of trees suitable for desert and arid climate zones is chosen and used to simulate the carbon sequestration and water demands of forests grown on dry land for the time period from 2030 to 2100. The widely used LUT Energy System Transition Model (LUT-ESTM)[18,19] is used to analyse the required energy sectors for afforestation projects in the appropriate locations and estimate the electricity, water and subsequently, carbon sequestration costs globally during the 70 yr period.

Land suitable for afforestation with demand for desalination

The extent of natural tree cover that would exist if human influence was not accounted for was previously estimated[20]. By removing the areas under human influence on the basis of available data, the global tree restoration potential was established and estimated to be up to 751 $GtCO_2$ of carbon sequestration potential on a total area of 9 million km^2. The land areas are those determined to have characteristics that support forest growth. Some of the restoration areas presented in ref. [20] lie in hydrological basins with arid conditions and low water use, or basins with high levels of water stress[21]. Since the above-mentioned water basins have low supplies of renewable water resources, the corresponding restoration areas are determined to be where desalination is required for the growth of trees (illustrated in Fig. 1a as 'Restoration land with desalination demand').

Areas with land cover that are neither primarily vegetation, cultivations or urban areas nor water bodies are labelled as bare areas[22]. These land cover areas, based on 2009 data[22], are overlapped with the water stress maps, as done for restoration land in the previous step. The resulting bare land areas with and without desalination demand are presented in Fig. 1a.

The approach of using seawater desalination to irrigate mature urban trees to offset carbon emissions was first modelled for the villa neighbourhoods of Abu Dhabi[23]. Building on this approach, a combination of eight tree species suitable for arid and tropical conditions were assumed for afforestation in the areas with desalination demand shown in Fig. 1b,c. Figure 1c shows the CO_2 sequestered by each of the chosen trees over the time period 2030–2100. The trees were distributed on the basis of shares that were validated with expected carbon stocks of mature boreal, temperate and tropical forests[24]. The carbon stored in the aboveground and belowground biomass, dead wood, litter and soil of the eight trees are accounted for in Fig. 1c and are based on the tree allometry and carbon sequestration equations provided in Supplementary Data 1. The global average CO_2 sequestration rate, based on the share of trees and average sequestration rates of forests (Supplementary Data 1), is shown on the right-axis of Fig. 1c. The water demand for the trees will be met through RE-based SWRO desalination from the nearest coastline. The water demand is proportional to the canopy area of the trees and is also a function of the location-specific reference evapotranspiration rate (ET_o) (Supplementary Fig. 4) and tree-specific water use as further explained in Methods[23]. Figure 1b shows the average daily water or desalination demand for the tree mix in all regions with afforestation potential in 2100 when the forests are mature. The regions excluded in Fig. 1b are those where the climate zone is not conducive for the selected tree mix (Supplementary Fig. 2, Table 1 and Note 1). Increase in tree cover is also expected to increase precipitation locally as modelled for afforestation projects in the Sahara Desert[25], where a maximum of 26% of the evapotranspiration is re-precipitated locally[26]. Recycling of increased precipitation due to increase in tree cover is taken into account, with an upper limit of 26% for all regions due to data limitations (Supplementary Fig. 4).

Costs of sequestering CO_2 through afforestation on arid land

The cumulative CO_2 sequestered from 2030 to 2100 if afforestation took place in the regions shown in Fig. 1b with the canopy cover available for restoration given in ref. [20] and bare land areas with a 20% canopy cover are shown in Fig. 2a. The world was divided into nine main regions used in the LUT-ESTM framework[18] and nations not within the framework were listed under the Rest of World category (Supplementary Data 1). Figure 2a shows that the Middle East and North Africa (MENA) region has the highest share of CO_2 sequestration potential of 131 $GtCO_2$ by 2070, followed by Sub-Saharan Africa with 87 $GtCO_2$. This potential is driven by the availability of restoration and bare land areas with demand for desalination in these regions. By 2070, when the trees are expected to be mature as noted in Methods, Europe and Eurasia have the least estimated potential with 3.4 $GtCO_2$ and 1.2 $GtCO_2$, respectively. This low potential is due to the low availability of land area within the temperature range suitable for the mix of trees. A secure supply of desalinated water for irrigation helps to ensure the survival and carbon sequestration of the tree mix.

Figure 2b captures the annual costs of irrigating and maintaining the restored forests in the areas shown on the map in Fig. 1b with RE-based SWRO over the 70 yr period. The presented annual historic CO_2 cost is explained in equation (5) in Methods. In the chart, the costs for countries with cumulative sequestration potential greater than 1 $GtCO_2$ by 2070 and the global total are shown. The bubble size represents the cumulative CO_2 sequestered for each of the countries. The global average decreases from approximately €457 per tCO_2 in 2030 to €99 per tCO_2 by 2100. The high costs at the start of the modelled transition are due to the low CO_2 capture rates, where the cumulative CO_2 sequestered worldwide in 2030 is estimated to be about 0.78 $GtCO_2$. Over time, the CO_2 sequestration costs for the countries shown converge towards the global average and these countries are responsible for over 90% of the global CO_2 sequestered by 2100. The costs for countries such as Afghanistan, Iran, Chad and Niger are higher than the global average due to the relatively higher water transportation distances. For instance, the weighted average vertical pumping distance of Iran is estimated to be 1,200 m, while the global average is about 590 m. Countries such as Spain, with carbon sequestration costs

Fig. 1 | Land, desalination demand and tree mix. a, Global distribution of land (restoration and bare land) for afforestation with desalination. The regions in black are those where neither restoration potential nor bare land can be found. For the land with restoration potential, ref. [37] estimates the continuous canopy cover of the trees which is the area of land that is covered by tree crown vertically projected to the ground. The range of tree canopy cover is 0–100% and allows to account for different tree covers around the world such as savannahs, woodlands and tropical forests (Supplementary Fig. 1). Bare land areas are assumed to have a potential canopy cover of 20%, which is set as the upper limit of bare land utilization in this research as further explained in Methods. **b**, Desalination demand per unit canopy area of the combination of the 8 trees by 2100; only those locations where temperature does not drop below 5 °C for more than 5 days are chosen. **c**, Cumulative CO_2 sequestered by each tree species over time (left-axis) and global average CO_2 sequestered per km^2 of land (right-axis) due to share of trees in the tree mix as presented in the validation worksheet of Supplementary Data 1. The combination of 8 trees is chosen due to the availability of data. However, a wider range of trees suitable for the specified climate can be used to create healthier, self-sustaining forests as explained in Methods.

https://doi.org/10.1038/s41893-022-01056-7

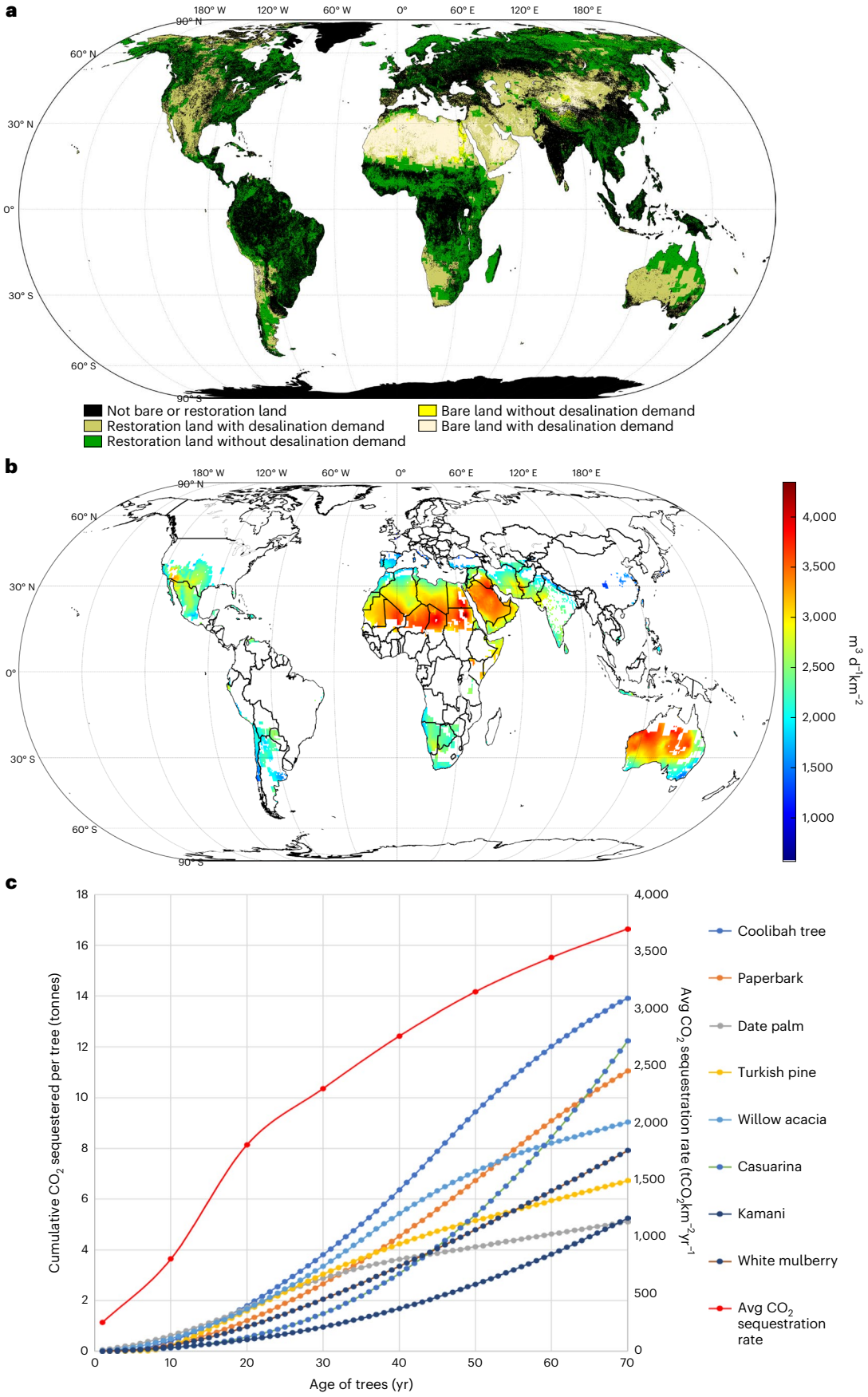

https://doi.org/10.1038/s41893-022-01056-7

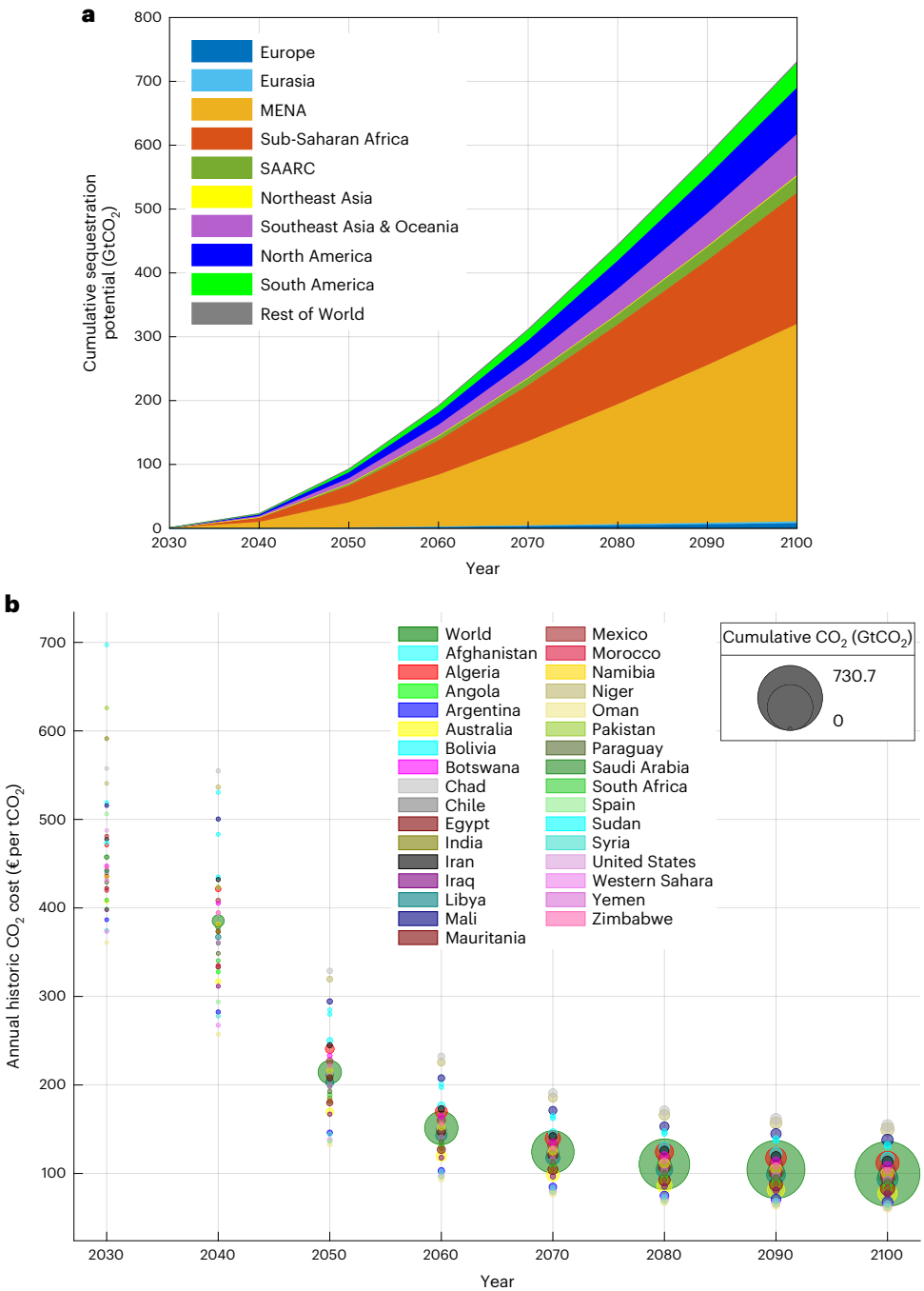

Fig. 2 | CO_2 sequestration potential and costs. a, Global cumulative CO_2 sequestration potential and for each major region. Potentials estimated for the land area suitable for afforestation with desalination in Fig. 1b and available restoration area as explained in Methods. The data are for the assumptions of bare land area use of 20% and temperature of 5 °C for 5 days. Countries that constitute the major regions are given in Supplementary Data 2. SAARC represents the South Asian Association for Regional Cooperation. **b**, Annual historic costs for the world and countries with large sequestration potentials (>1 $GtCO_2$ by 2070).

at €54 per tCO_2 by 2100, have lower transportation costs but also lower desalination demand per tonne of carbon due to the lower reference evapotranspiration coefficient. The global average water demand per tonne of CO_2 is 198 m^3, while for Spain it is 129 m^3. Variation in costs for the major regions is given in Supplementary Fig. 5.

The annualized costs of the total system (energy, desalination, irrigation and land systems) that comprise the costs in Fig. 2b are shown in Fig. 3a and broken down on a major region basis. The corresponding average annual CO_2 sequestration potential for the major regions is illustrated in Fig. 3b. Reflecting the high annual sequestration potentials in the regions, MENA and Sub-Saharan Africa also accounted for the largest annualized costs. After 2050, the reduction in annualized costs is driven by the decommissioning and re-installation of lower-cost solar photovoltaics (PV), wind and battery technologies. Water transportation infrastructure costs constitute the largest share of the annual costs for all regions.

The carbon sequestration costs for the period from 2030 to 2100 were modelled globally at a spatial resolution of 0.5° × 0.5°. Further details on the LUT-ESTM framework and corresponding analysis are provided in Methods. Figure 3c presents the annual historic CO_2 costs

https://doi.org/10.1038/s41893-022-01056-7

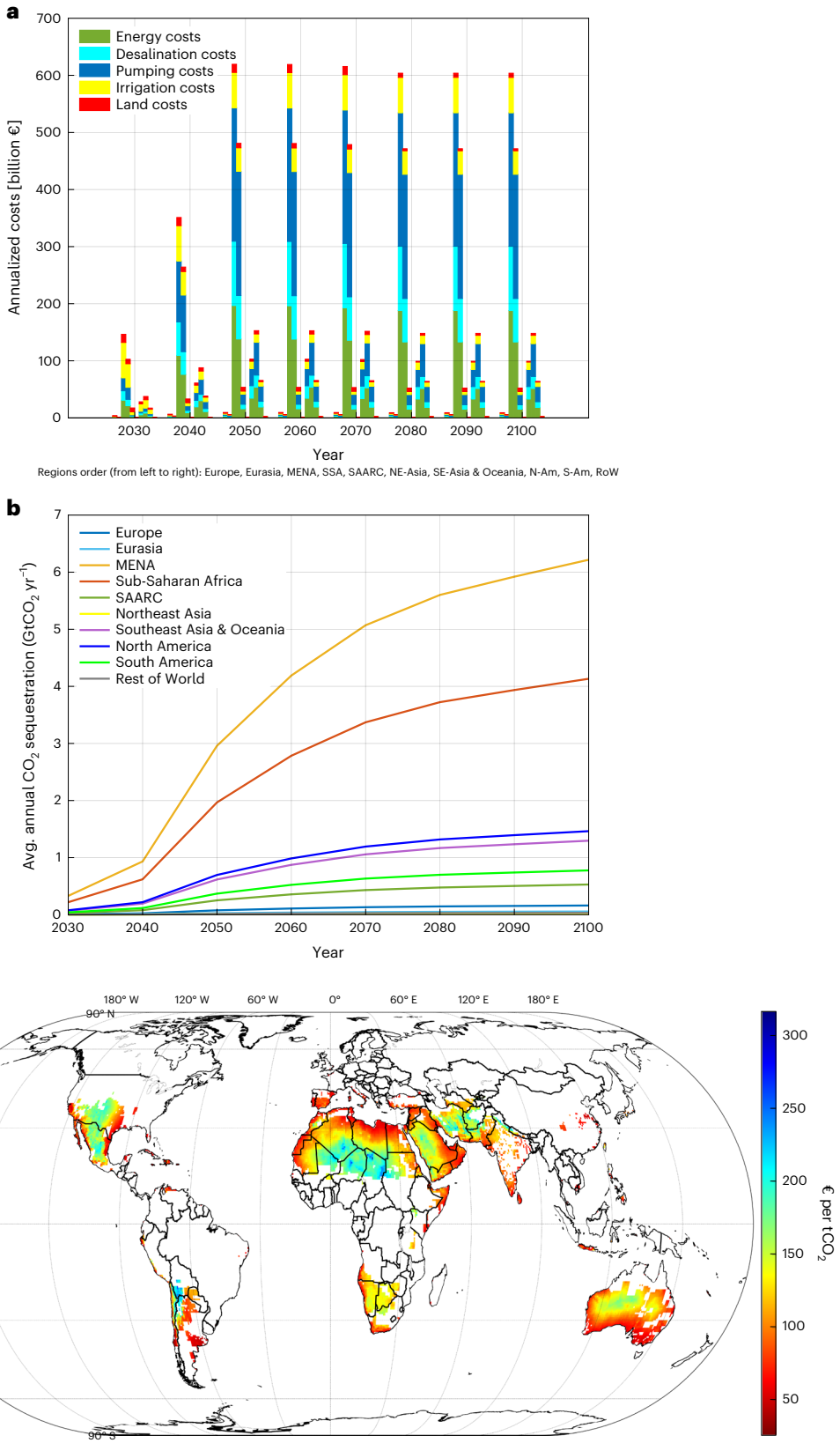

Fig. 3 | Afforestation costs breakdown. a, Annualized costs for the complete system for all nine major regions and time period. By mid-century, the global annualized costs are expected to be €1,499 billion for an annual sequestration of 7 $GtCO_2$ and decreases slightly to €1,462 billion towards the end of the century for an annual sequestration of 14 $GtCO_2$. **b**, Corresponding average sequestration rates for all the major regions over time. **c**, Annual historic CO_2 cost for the year 2070 for all regions with desalination demand and afforestation potential.

determined for the year 2070 of the modelling period. The map shows that nodes with afforestation potential closer to the coastline have a CO_2 cost range of €50–100 per tCO_2, while the global range is from about €20–300 per tCO_2. Detailed country specific results are provided in Supplementary Data 2 and global maps for 2050 and 2100 are provided in Supplementary Fig. 6.

RE-based desalination for afforestation in arid areas

The global average levelized cost of electricity (LCOE) of the energy system for continued water supply for irrigating the forests, including the energy for desalination and water pumping, decreases from €46.9 MWh^{-1} in 2030 to €31.0 MWh^{-1} by 2100. Due to the lack of data to project costs, the cost of system components post-2050 is assumed to be the same as in 2050. However, further decline in RE costs can be expected after 2050, driving down the costs of the final system. By 2050, countries with CO_2 sequestration potential have more than 80% of the corresponding electricity generation from solar PV, highlighting the high solar irradiation levels in regions with afforestation potential. Battery storage is used to complement solar PV generation during times of low solar insolation, meeting up to 67% of the global electricity demand. Figure 4b illustrates the levelized cost of water (LCOW) for producing and transporting desalinated water to afforestation sites for the year 2070. The cost of water production is mostly in the range of €0.15–0.56 m^{-3} and is higher in the nodes further away from the coastline. The global average LCOW decreases from €0.59 m^{-3} to €0.44 m^{-3} during the 70 yr period.

The energy required to run the desalination plants accounts for approximately 52% of the total energy demand, while the remaining 48% is to pump the water. For countries such as Tajikistan and Chile, water pumping accounts for more than 70% of the total energy demand. In contrast, countries with shorter pumping distances, such as Qatar and Vietnam, use less than 10% of the total energy demand for pumping. Figure 4c shows that the energy demand per unit tonne of average annual CO_2 sequestered, on a global average, stabilizes at around 1 MWh per tCO_2 by 2100 for the proposed system. The minimum–maximum interval indicates that countries can have more or less than this average. The peak in 2040 is due to the increase in energy demand as growing trees require more water but still have lower carbon sequestration potential, with energy demand starting to decline as carbon sequestration potential increases. The energy demand decreases to almost 1 MWh per tCO_2 by 2100, while for some countries it is even less, as shown by the red shaded area. Pumping energy demand accounts for almost half of the total average, while in some countries the pumping energy demand is minimal, as shown by the lower end of the blue area. In 2070, the ten countries with the largest CO_2 sequestration potential accounting for 65% of the global potential (Algeria, Australia, Egypt, Libya, Mauritania, Mexico, Niger, Saudi Arabia, Sudan, the United States) have energy efficiency use values of 1–1.5 MWh per tCO_2. The pumping distances shown in Supplementary Figs. 7–11 capture more details on the global system. Table 1 summarizes key features of the global energy system required during the lifetime of the forests for the years 2030, 2050, 2070 and 2100.

Comparing major carbon dioxide removal options

In Table 2, the features of the CDR options proposed in this research are compared with those of the main CDR options currently used in IAM models: direct air capture and carbon capture storage (DACCS) and bioenergy and CCS (BECCS). BECCS has historically been the dominant CDR technology due to the perceived lower costs, ability to generate electricity and provide flexibility to the energy system. However, the increasing limitations of water and land constrain the deployment of BECCS[27–30]. Meanwhile, the projected decreasing costs and potential of DACCS have made the technology an increasingly attractive CDR option[27,31].

The costs for afforestation shown above post-2050 can be expected to decrease further due to the declining RE costs. Based on the data in Table 2, by mid-century, DACCS at approximately €100 per tCO_2 may be a cheaper CDR option than desalination-based afforestation. However, on a country basis, as shown in Fig. 3c and Supplementary Data 2, afforestation with RE-based SWRO may be a more cost-effective solution, with the added benefits of restoring land. For the case of the green wall restoration project in the Sahel region, a dollar invested in the restoration of degraded land is found to yield economic returns of US$1.1–4.4 (ref. [32]). The median economic benefits in the Sahel region due to restored forests are estimated to be US$215,200 km^{-2}. The benefits of forest restoration on arid lands are not within the scope of this research, but if included, will further bring down the costs for desalination-based afforestation in some regions. A key drawback of desalination-based afforestation is the approximately 20 yr time delay after the investment to benefit from a substantial CO_2 sequestration rate as shown in Fig. 3b. This delay and uncertainty impede the planning of climate mitigation portfolios for different regions.

In Supplementary Data 1, we present further analysis of the contribution of afforestation with RE-based SWRO to climate change mitigation efforts considering a future scenario where the global energy system achieves zero emissions by 2050.

Discussion

The goal of this work is to highlight the untapped afforestation potential on arid lands to support tree growth and provide a substantial CDR opportunity, provided there is a secure supply of water. While the initial costs of such a system are high (a global average of €457 per tCO_2), the increasing carbon sequestration potential of the trees and decreasing cost of renewable electricity make such projects competitive with CDR options such as DACCS and BECCS. Forests also help fight the increasing threats of desertification, soil erosion and floods, and help fix the water cycle. By mid-century, about 0.26 $GtCO_2$ could be sequestered annually through afforestation with RE-based SWRO at annual historic costs of €50–100 per tCO_2. By the end of the century, the number rises to 6.7 $GtCO_2$ for the same cost range. Solar PV and wind enable the production of low-cost desalinated water and thereby create opportunities for afforestation in arid regions. An increase in precipitation due to the tree canopy cover, which has not been accounted for in detail due to the lack of available data, will further drive down these costs as water is the key cost component[25]. It has to be noted that areas of restoration where water is not an issue will provide the cheapest carbon sequestration opportunities.

Issues with large quantities of concentrated brine currently being discharged into the marine environment—an estimated 142 million $m^3\ d^{-1}$—from the global desalination capacity of 95 million $m^3\ d^{-1}$ have been highlighted[33]. This leads to the pollution of coastal waters and damage to sensitive marine life, which will deteriorate as the global desalination capacity increases. Brine management of desalination plants is of crucial relevance for overall sustainability. An increasing area of interest is the recovery of minerals from concentrated brine discharge to meet the increasing global demand for critical elements while creating new economic opportunities for the regions[33,34]. In addition to mineral recovery, existing industrial processes can be used to extract chemicals such as sodium hydroxide and hydrochloric acid, which are used within the desalination plants themselves and in other various applications[35]. The use of treated brine discharge as an unconventional water source for the copper industry in Chile has also been demonstrated[36]. The use of brine discharge will further contribute to the reduction in costs of desalinated water.

There are several limitations to this study, namely the projection of carbon sequestered in forests, the diversity of trees and the water demand of forests. The data chosen for this study were validated through different approaches (Supplementary Data 1) to try to best simulate mature forests with sufficient water supply. Similarly, the

https://doi.org/10.1038/s41893-022-01056-7

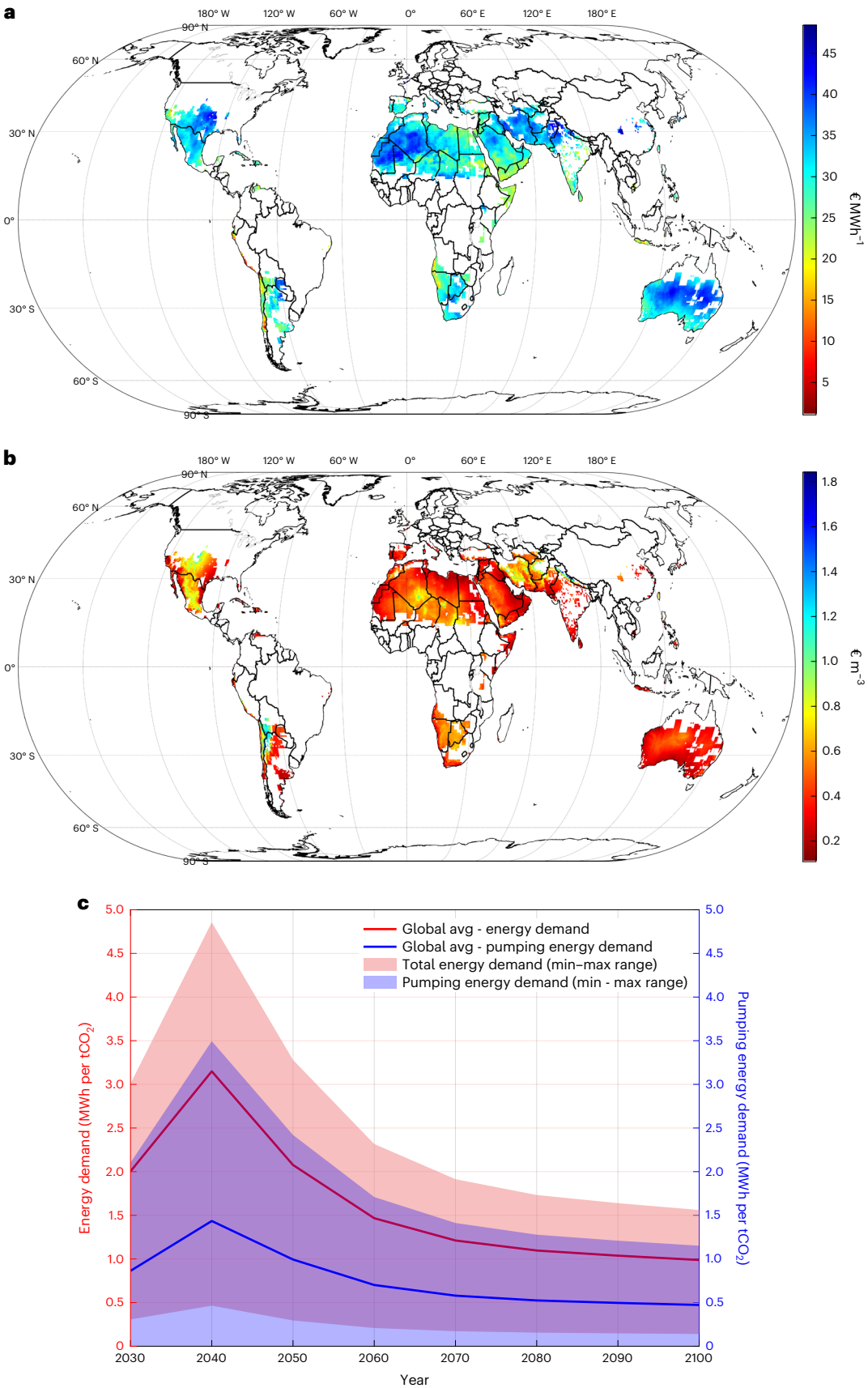

Fig. 4 | LCOE, LCOW and energy demand variation. a, LCOE values for nodes with afforestation potential for the year 2070, including solar PV and battery for near to baseload SWRO desalination and water pumping supply. **b**, Corresponding LCOW values for the year 2070. **c**, Average energy demand and pumping demand of all countries during the time period 2030–2100.

Table 1 | Key features of the global energy system for the years 2030, 2050, 2070 and 2100

		2030	2050	2070	2100
PV capacity	TW	1.0	10.7	10.7	10.7
Wind capacity	GW	58.9	153.5	149.5	149.3
PV generation	TWh	1,912	19,664	19,657	19,655
Wind generation	TWh	167	443	432	431
Battery storage capacity	GWh	2,453	25,403	25,421	25,423
Desalination capacity	$m^3 d^{-1}$	7.73×10^8	7.98×10^9	7.98×10^9	7.98×10^9

Detailed numbers for all years and countries are provided in Supplementary Data 2.

Table 2 | Comparison of the data from this research with those of DACCS (low-temperature DAC) and BECCS

		Afforestation with RE-desalination	DACCS (low-temperature DAC)	BECCS
Cumulative global potential	$GtCO_2$	92 (2050) 730 (2100)	no obvious limit	178–1,170 (sustainable potential is lower)
Average global CO_2 sequestration rate	$GtCO_2 yr^{-1}$	7 (2050) 14 (2100)	8 (CDR demand in 2050) 37 (peak deployment in 2100)	sustainable deployment: 3–5 $GtCO_2 yr^{-1}$
	$MtCO_2 km^{-2} yr^{-1}$	0.002 (2050) 0.005 (2100)	2.5 (2050)	0.003–0.002 (2100) 0.0025–0.0004 (current)
Average cost (range)	€ per tCO_2	214 (2050) 99 (2100)	54 (2050; in regions with solar and wind conditions akin to the Maghreb region) for DACCS: CO_2 transport and storage may be €45 per tCO_2 (near-term) and €30 per tCO_2 (long-term)	100–200 (expected to increase after 2050 due to land and water limitation)
Water demand	m^3 per tCO_2	416 (2050) 198 (2100)	no water use, in case of Climeworks plant water produced as a by-product, estimated value of 2.03	60 (if only additional water considered; includes water for CCS); 540 (when all water is provided through irrigation)
Energy demand efficiency	MWh per tCO_2	2.1 (2050) 1.0 (2100)	0.8–1.0 (2050)	1.5–6.0 (useful final energy output)
Land demand efficiency (excluding energy land use for last two options)	km^2 per $MtCO_2$	356 (2050) 192 (2100)	0.4 (current value from Climeworks plant)	314–578 (2100) 400–2,400 (current)

The data for the features for DACCS and BECCS were obtained from available literature. DACCS would have an additional cost and energy demand due to the need to store the captured CO_2. The year for the data is provided in brackets[3,27,29,31,62,63].

relationship between increased precipitation and tree canopy cover in different regions needs to be better understood. Not all the land shown in Fig. 1b may be restored, but the results present a theoretical potential which is in line with the global potential values from ref. [37]. Some of this land may in fact be converted to agricultural land or suffer the severe effects of climate change such as forest fires and floods. Furthermore, the current canopy cover for the nodes in the study is limited by existing data, but may have different values in practice, thereby influencing the carbon sequestration potential and water demand. The bare land areas may also be further studied and the canopy cover varied. Restoration of forests in cooler climates such as the boreal zones of North America and Europe, as shown in Fig. 1a, which can further contribute to the CO_2 sequestration potential, and the corresponding impacts on climate change mitigation are not considered in this research.

Rotenberg and Yakir[38] explain, on the basis of experiments in the semi-arid planted forest Yatir in Southern Israel, that forests in stable high radiation load and low cloud conditions result in an increase in radiation load. The authors suggest that it would take decades before the biogeochemical cooling effects of CO_2 sequestration can overcome the biogeophysical warming effects, decreasing the carbon sequestration potential of the forests. In contrast, Yosef et al.[39] show, using the same data coupled with a land-atmosphere model, that large-scale restoration of forest ecosystems in the Sahel region and Australia leads to a local cooling effect. The impact of cooling through carbon sequestration would overcome biogeophysical warming in about 6 yr. The 'breakeven' point for biogeophysical and biogeochemical aspects of afforestation on arid lands has been assessed and the lack of moisture has been determined to be the key driver of the increase in the radiative load at the sites[40]. Afforestation on arid lands with a reliable supply of desalinated water presents a new angle to this discussion and the corresponding biogeophysical impacts have to be further investigated.

Another question that arises with desalination-based afforestation is what happens after the 70 yr time: will there be a need to maintain the forests continuously or will the forests be self-sufficient and no longer require investments? Shall the new forests be further developed as natural ecosystems for various species or rather as economic forests even with a BECCS option? What measures are required to ensure as high and long-term carbon storage security as possible? Forest fires, for instance, have increased by 13% in 2020 relative to 2019, although 75% of the forest fires were caused by human activity[41]. Hotter and drier climates, coupled with land conversion to agriculture and poor forest management, have resulted in forests being more susceptible to fires. The Middle Eastern Green Initiative[42] is the largest afforestation project established in 2021, with the goal of rehabilitating land in the region through the planting of 50 billion trees suitable for local conditions and the perceived benefits of reduction in desertification rates, soil erosion, sandstorms and lowering of local temperature, making the region more liveable for its citizens. Do these benefits outweigh the costs of maintaining forests over a long period? These questions require further detailed investigation. Furthermore, existing research suggests that

there is a substantial amount of dust plume from the Sahara arriving in the Amazon that may contribute to the productivity of the Amazon rainforest[43,44]. Dust plumes are not yet well understood and the impact of afforestation areas on dust plumes have not yet been modelled. As such, the relationship between dust plumes, the productivity of the Amazon rainforest and afforestation on arid lands has to be investigated.

On a global average, the pumping infrastructure costs contribute almost as much as the energy system costs to the final system (Supplementary Data 2). This may be further tuned by adopting better costs for pumping and piping on long distances where there may be an economy-of-scale effect. In this research, however, the pumping and piping costs were extrapolated proportionately with distance. It has to be noted that for smaller countries such as the United Arab Emirates and Israel, the energy system still plays the key role in the cost structure. Afforestation sites that are further inland bear higher costs due to the pumping infrastructure and pumping energy demand. In parts of Iran, USA, Mexico and Chile, the total energy demand ranges between 0.010 and 0.021 MWh m^{-3}, while the global average is estimated to be 0.005 MWh m^{-3} (Supplementary Fig. 18 and Data 2). Based on literature[45], the option of desalinating and transporting water to these regions may still be more viable than using atmospheric water generators, as explained in Supplementary Fig. 18. In addition, the weighted average cost of capital (WACC) chosen in this study for all regions was 5%, assuming stable conditions in the country. This will vary with countries over time and due to the lack of data projection, a WACC of 5% was used.

In 2019, the company Terraformation carried out a pilot project to restore arid and degraded land in Hawaii using solar-powered desalination plants[46]. The company seeks to scale up native ecosystem restoration projects as a low-cost carbon capture solution. Another example of afforestation in arid lands are the forests being grown in Luxor, Egypt using treated wastewater[47]. The results of this research expand on and further support these global initiatives to restore forests on arid lands, not as plantations but as forests that grow undisturbed. The importance of using an optimized portfolio of CDR options that look beyond just the techno-economic feasibilities to determine the best pathways to limit global temperature rise has been previously discussed[2]. Renewable electricity-based desalination for afforestation may emerge as a major CDR option next to DACCS given the comparable cost in the longer term but substantial co-benefits for large regions in the global sunbelt.

Methods

Land area for afforestation with RE-based SWRO desalination

Restoration land[37] and bare land areas[22] with the following water stress conditions were determined to be areas where forests could grow if irrigated with a secure water supply. The projected water stress, water supply and demand data for the decade 2040 are used. The renewable water resources in these areas were not considered sufficient to sustain forest growth.

- Land nodes that lie in high (40% < WS <80%) and extremely high water stress basins (WS > 80%)
- Land nodes that lie in low water stress basins (WS < 10%) but have low water supply (<10 cm)
- Land nodes that lie in arid and low water use basins (water demand < 3 cm and water supply < 10 cm)

Restoration land potential accounts for several environmental variables of soil, climate and topographic layers. The corresponding tree canopy covers for all the restoration nodes (Supplementary Fig. 1) were set to be the maximum area of the nodes that can be afforested.

Bare land data were obtained from the 2009 land cover map[22]. The maximum canopy cover assumed for bare land nodes was 20%, which is an estimate of the global average of the restoration data. In this data set, environmental variables suitable for forest cover were not considered. This may impact the tree canopy cover possible on these lands. Nevertheless, if there is a secure water supply, the tree canopy cover on the bare lands could be higher than 20% and warrants further research. Reflecting this approach, Egypt is a country where the reclamation of desert land has been carried out with expectations to convert more than 7% of desert to arable land, but this effort has been hindered by the lack of water resources[48]. In this research, the intention is to use available bare land within a limit, given reliable water supplies.

The tree mix chosen for this study is suitable for desert or tropical conditions. Thus, the restoration areas and bare land areas with afforestation potential but with inconducive climates were excluded. The suitable areas were extracted by considering the corresponding climatic zone, the US Department of Agriculture hardiness zone and the subsequent temperature range that suits all trees. The suitable temperature range was determined to be all places where the temperature does not drop below 5 °C for more than 5 days (Supplementary Fig. 2, Table 1 and Note 1).

Supplementary Fig. 3 presents an outline of the overall concept of this study. Supplementary Fig. 4 is a flowchart illustrating the overall approach taken in this study and provides a framework for the methods outlined below.

Plotting CO_2 sequestration of trees

The following trees were chosen on the basis of data from refs. [23,49] and the Centre for Urban Forest Research (CUFR) tree carbon calculator:

1. Coolibah tree
2. Paper bark
3. Date palm
4. Turkish pine
5. Willow acacia
6. Iron wood
7. Kamani
8. White mulberry.

The allometry equations to define all trees, except date palms, were verified from the Urban Tree Database[49]. It has to be noted that in the case of high-density forests, the allometry equations may differ from those of urban trees, which would have sufficient space to grow. However, given the availability of data, the urban growth equations were used as in Supplementary Data 1. The CO_2 sequestration rates were based on the data in the CUFR calculator for the tree species when grown in tropical or desert climate zones (Supplementary Data 1). The data from the CUFR calculator provide the aboveground and belowground biomass stored for the individual tree types. The carbon pools, soil, litter and dead wood were accounted for on the basis of estimates from the literature (Supplementary Data 1). It has to be noted that urban trees grow under good conditions and are maintained as opposed to forests[49]. In this research, the trees are intended to be irrigated and maintained regularly to ensure the productivity and self-sustainability of the forests.

The Urban Tree Database[50] explains that there are gaps in the data for date palms due to the lack of measurements. Thus, the corresponding aboveground and belowground biomass values were obtained from ref. [51], which measured and developed allometric equations for date palm species on arid land.

In a high-density, multispecies forest, trees grown will be healthier and have a higher carbon sequestration potential[50]. To emulate forest sequestration potentials, the ratio of the trees of each type in a unit area was varied such that the maximum annual carbon stored (tC ha^{-1} yr^{-1}) is similar to that of a mature tropical forest. A tropical forest was assumed since such forests would generally not have a lack of renewable water resources. The validation of the carbon sequestration data was carried out in the respective worksheet of Supplementary Data 1 using the share of the 8 tree species specified. Mature trees were considered to be 40 yr in this study, while the range found in the literature could be 20–70 yr.

Equations (1) and (2) illustrate the method to determine the cumulative carbon sequestered over time for each land node with afforestation potential and the corresponding total country value:

$$\mathrm{TotalCarbon}_{\mathrm{node,yr}} = \sum_{\mathrm{type}=1}^{8} \mathrm{Node}_{\mathrm{area}} \times \mathrm{TreeShare}_{\mathrm{type}} \times \mathrm{TreeDensity} \times \mathrm{TreeCarbon}_{\mathrm{type,yr}} \quad (1)$$

$$\mathrm{CountryCarbon}_{\mathrm{yr}} = \sum_{\mathrm{node}=1}^{\mathrm{total\ aff.nodes}} \mathrm{TotalCarbon}_{\mathrm{node,yr}} \quad (2)$$

where $\mathrm{Node}_{\mathrm{area}}$ is the total afforestation area available in the node[21,22,37], $\mathrm{TreeShare}_{\mathrm{type}}$ is the percentage share of the tree type from the total mix of trees, $\mathrm{TreeCarbon}_{\mathrm{type,yr}}$[49–55] is the cumulative carbon sequestered by the tree type by a specific year and total aff. nodes is the total number of land nodes with afforestation available in the country. $\mathrm{TreeCarbon}_{\mathrm{type,yr}}$ was obtained from the data in Supplementary Data 1 where the cumulative CO_2 stored over the 70 yr period is presented for all 8 tree species. The data on the shares of the tree types are also presented in Supplementary Data 1.

Water demand of the tree mix

The water demand for the tree types are a function of the reference ET_o of the location, the tree species' corresponding water use coefficient in the region type and the efficiency of the irrigation equipment used[23]. The global ET_o data were obtained from the FAO Map Catalog[56], the data being the average values from the time period 1961–1990 in 0.16° × 0.16° resolution. The water use coefficients are specific to the tree species and region type, and is a share of the ET_o (Supplementary Fig. 5). Equations (3–5) present the method used to determine the water demand for every afforestation node in a year, and the corresponding water demand for the country.

$$\mathrm{TotalWater}_{\mathrm{node,yr}} = \sum_{\mathrm{type}=1}^{8} \Big(\mathrm{Node}_{\mathrm{area}} \times \mathrm{TreeShare}_{\mathrm{type}} \times \mathrm{TreeDensity} \times \mathrm{WaterDemand}_{\mathrm{type,yr}} \times \mathrm{Coefficient}_{\mathrm{type}} \times \mathrm{Eto}_{\mathrm{node}} \times \frac{1}{\mathrm{IrrigEfficiency}} \times \mathrm{AreaIrrigated}\Big) \quad (3)$$

$$\mathrm{Final\_TotalWater}_{\mathrm{node,yr}} = \mathrm{TotalWater}_{\mathrm{node,yr}} \times (1 - \mathrm{RecyclyingShare(yr)}) \quad (4)$$

$$\mathrm{CountryWater}_{\mathrm{yr}} = \sum_{\mathrm{node}=1}^{\mathrm{total\ aff.nodes}} \mathrm{Final\_TotalWater}_{\mathrm{node,yr}} \quad (5)$$

where $\mathrm{WaterDemand}_{\mathrm{type,yr}}$ is the water demand of an individual tree type in a specific year, $\mathrm{Coefficient}_{\mathrm{type}}$ is the tree species' specific water-use coefficient, $\mathrm{Eto}_{\mathrm{node}}$ is the reference evapotranspiration rate for the afforestation node, IrrigEfficiency is the efficiency of the sub-surface drip irrigation (95% in this study), AreaIrrigated is the maximum share of the afforestation area that is irrigated (90% in this study), $\mathrm{Final\_TotalWater}_{\mathrm{node,yr}}$ is the final water demand taking into account precipitation, RecyclyingShare(yr) is the share of the evapotranspiration that is precipitated and is dependent on the year, $\mathrm{CountryWater}_{\mathrm{yr}}$ is the total water demand for the afforestation area in the country and year.

The irrigation equipment used are the high-efficiency sub-surface drip irrigation systems that have been used in Oman to irrigate date palm plantations[57] and in Texas for crops such as corn, cotton and soybean[58]. The details of the irrigation system used are provided in Supplementary Data 1. The increase in water demand is proportional to the canopy area of the trees[23,59]. Once the total canopy area of the trees in an afforestation node is equal to the maximum afforestation area of the node, the water demand is set to not increase. The increasing canopy cover also results in an increase in precipitation, which has been estimated and accounted for as recycling in Supplementary Fig. 6 (refs. [25,26]). This is applied to the water demand obtained in equation (3) to account for precipitation recycling over time as shown in equation (4). The competition for local water resources from local vegetation, which may increase the final water demand, is not considered. The use of highly efficient sub-surface drip irrigation systems to deliver water directly to the trees for the full period of 70 yr, coupled with the possible increase in precipitation as the trees mature, is intended to ensure that the water demand of the trees is always met.

LUT Energy System Transition Model

The LUT-ESTM[18,19] has been used extensively to analyse energy system transition pathways towards entirely RE-based energy systems on a global, regional and country basis. In this study, a simplified version of the model[15] is used to cost-optimize the energy system for the SWRO desalination plants necessary for afforestation for the time period 2030–2100. The optimization is carried out in an hourly temporal resolution and a 0.5° × 0.5° spatial resolution. Supplementary Figs. 14 and 15 illustrate the LUT-ESTM set up and flow of steps in this study, respectively. The electricity is generated by solar PV and wind power plants on the basis of the RE resources. Battery storage and power-to-gas components are used to complement the electricity generation sources, ensuring cost-optimal operation of the SWRO plants.

The financial and technical parameters of all energy system components used in this research up to 2050 are varied according to specific data sources and presented in ref. [60]. These parameters include the capital costs, operating costs, lifetime and efficiency values. However, due to the lack of projection data after 2050, the parameters of all components are kept the same as at 2050. Similarly, the parameters for the SWRO desalination system, water pumping and piping are obtained from ref. [15] where all relevant references are presented. On the basis of the lifetime of all system components, the components are decommissioned and replaced during the period 2030–2100. It has to be noted that the fixed operating costs for the SWRO desalination plants account for maintenance and replacement of membranes, assuming an annual replacement rate of 15%. The SWRO desalination plants, pumps and pipes are decommissioned on the basis of their respective lifetimes.

The results of the model were used to calculate the LCOE, LCOW and CO_2 sequestration costs for all nodes with afforestation potential during the 70 yr period. Final results on a country basis are presented in Supplementary Data 2. The CO_2 costs also accounted for the land rent, conversion costs, monitoring costs, operation and maintenance (O&M) costs and fertilizer costs as shown in Supplementary Data 1 and 2. These costs were obtained from ref. [4] where data are provided in a regional format. The capital and operating costs of sub-surface drip irrigation equipment and the decommissioning costs during the period 2030–2100 were also accounted for.

The model opts to run the SWRO desalination plants at high full load hours to minimize the costs[61]. This means that due to the variable nature of solar and wind resources, there are higher RE capacities installed than required for some hours of the year, as it is cheaper to curtail the energy than increase storage. For the modelled system, this results in a global average electricity excess of about 24% of the total demand. However, in a more efficient sector-coupled energy system, this excess would be used by other sectors to their advantage[18,19]. As such, an excess limit of 10% was specified. The excess electricity was considered to be sold to the other sectors at the LCOE of the energy system for that year, and the income accounted for in the final system LCOE (Supplementary Fig. 12 and observable in further detail in Supplementary Data 2).

The land use of the ground-mounted single-axis tracking PV, the fixed-tilted PV and onshore wind power plant capacities modelled in

this study were determined using current and projected power densities. The projections accounted for improvements in the efficiency of the technologies. The power density values and corresponding land use data are shown in Table 2 and Supplementary Fig. 17, respectively, with more details in Supplementary Data 2.

Annual historic CO_2 cost

The annual historic CO_2 cost is the annualized cost of running the energy, desalination, irrigation and land for that year and the annual average CO_2 sequestration rate.

$$\begin{aligned}&\mathrm{AnnHistoric}_{\mathrm{node,yr}} = (\text{annualized costs of energy system in operation}\\&+\text{annualized cost of desalination sytem in operation}\\&+\text{annualized costs of irrigation system in operation}\\&+\text{annualized cost of land})\\&/\text{average } CO_2 \text{ sequestration rate in decade}\end{aligned} \tag{6}$$

where all annualized costs are in billion euros for the year and average CO_2 sequestration rate is in $GtCO_2\,yr^{-1}$ for the specific node. All costs for the countries modelled can be found in Supplementary Data 2. The financial and technical parameters for the desalination and energy system can be found in ref. [60], the irrigation system details are provided in Supplementary Data 1 and the land costs are provided in Supplementary Fig. 13. As explained in the Discussion, a WACC of 5% was used for all countries.

The annualized costs of the energy system, desalination system, irrigation and land systems for a specific node and year are described in equations (7–10), respectively.

$$\begin{aligned}&\mathrm{AnnualisedEnergySystemCosts}_{\mathrm{node,yr}}\\&=\sum_{\mathrm{et}=1}^{\mathrm{Etech}}(\mathrm{Capex}_{\mathrm{et}}\times\mathrm{crf}_{\mathrm{et}}+\mathrm{opexfix}_{\mathrm{et}})\times\mathrm{Cap}_{\mathrm{et}}+\mathrm{Egen}_{\mathrm{et}}\times\mathrm{opexvar}_{\mathrm{et}}\end{aligned} \tag{7}$$

where 'et' represents each of the energy system components, Etech is the total number of energy system components, $\mathrm{Capex}_{\mathrm{et}}$ is the capital expenditure of each energy system component, $\mathrm{crf}_{\mathrm{et}}$ is the capital recovery factor for each energy system component, $\mathrm{opexfix}_{\mathrm{et}}$ is the fixed operational expenditure of each energy system component, $\mathrm{Cap}_{\mathrm{et}}$ is the operating capacity of each energy system component, $\mathrm{Egen}_{\mathrm{et}}$ is the electricity generation of each energy system component and $\mathrm{opexvar}_{\mathrm{et}}$ is the variable operational expenditure of each energy system component.

$$\begin{aligned}&\mathrm{AnnualizedDesalSystemCosts}_{\mathrm{node,yr}}=\sum_{dt=1}^{\mathrm{Dtech}}(\mathrm{Capex}_{\mathrm{dt}}\times\mathrm{crf}_{\mathrm{dt}}+\mathrm{opexfix}_{\mathrm{dt}})\\&\times\mathrm{Cap}_{\mathrm{dt}}+(\mathrm{Capex}_{\mathrm{vp}}\times\mathrm{crf}_{\mathrm{vp}}+\mathrm{opexfix}_{\mathrm{vp}})\times\mathrm{Water}_{\mathrm{node}}\times\mathrm{Vertical}_{\mathrm{node}}\\&+\left(\mathrm{Capex}_{\mathrm{hp}\times\mathrm{crf}_{\mathrm{hp}}+\mathrm{opexfix}_{\mathrm{hp}}}\right)\times\mathrm{Water}_{\mathrm{node}}\times\mathrm{Horizontal}_{\mathrm{node}}\end{aligned} \tag{8}$$

where dt represents each of the desalination system components (SWRO desalination plants and water storage), Dtech is the total number of desalination system components, $\mathrm{Cap}_{\mathrm{dt}}$ includes the annual water production from SWRO desalination and water storage for the node, vp are the vertical pumping components, $\mathrm{Water}_{\mathrm{node}}$ is the annual water transported to node, hp are the horizontal pumping components, $\mathrm{Vertical}_{\mathrm{node}}$ is the average elevation for the node from the nearest coastline and $\mathrm{Horizontal}_{\mathrm{node}}$ is the horizontal water pumping distance for the node from the nearest coastline.

$$\begin{aligned}&\mathrm{AnnualizedIrrigationCosts}_{\mathrm{node,yr}}\\&=(\mathrm{Capex}_{\mathrm{it}}\times\mathrm{crf}_{\mathrm{it}}+\mathrm{opexfix}_{\mathrm{it}})\times\mathrm{Area}_{\mathrm{node,yr}}\end{aligned} \tag{9}$$

where 'it' represents the sub-surface drip irrigation system, $\mathrm{Area}_{\mathrm{node,yr}}$ is the afforestation area for each node

$$\begin{aligned}&\mathrm{AnnualizedLandCosts}_{\mathrm{node,yr}}\\&=(\mathrm{Conversion}_{\mathrm{node,yr}}\times\mathrm{crf}_{\mathrm{node,yr}}+\mathrm{LandRent}_{\mathrm{node,yr}}\\&+\mathrm{Monitoring}_{\mathrm{node,yr}}+\mathrm{O\&M}_{\mathrm{node,yr}}\\&+\mathrm{Fertilizer}_{\mathrm{node,yr}})\times\mathrm{Area}_{\mathrm{node,yr}}\end{aligned} \tag{10}$$

where $\mathrm{Conversion}_{\mathrm{node,yr}}$ is the land conversion cost in the specific node, $\mathrm{LandRent}_{\mathrm{node,yr}}$ is the annual land rent for the specific node, $\mathrm{Monitoring}_{\mathrm{node,yr}}$ is the monitoring cost for the forests, $\mathrm{O\&M}_{\mathrm{node,yr}}$ is the operation and maintenance cost and $\mathrm{Fertilizer}_{\mathrm{node,yr}}$ is an annual fertilizer cost. Equation (11) is used to determine the capital recovery factor for all system components.

$$\mathrm{crf}_t=\frac{\mathrm{WACC}\times(1+\mathrm{WACC})^{\mathrm{Nt}}}{(1+\mathrm{WACC})^{\mathrm{Nt}}-1} \tag{11}$$

where WACC is the weighted average cost of capital, *t* is the system component and Nt is the lifetime of the system component.

Data availability

Datasets used in this study were accessed from publicly available sources. All the data supporting the findings of this study are referenced within the manuscript and in Supplementary Information.

Code availability

Matlab scripts used in the analyses are available from the corresponding author on reasonable request.

References

1. IPCC *Climate Change 2022: Mitigation of Climate Change* (eds Shukla, P. R. et al.) (Cambridge Univ. Press, 2022).
2. Rueda, O., Mogollón, J. M., Tukker, A. & Scherer, L. Negative-emissions technology portfolios to meet the 1.5 °C target. *Glob. Environ. Change* **67**, 102238 (2021).
3. Smith, P. et al. Biophysical and economic limits to negative CO_2 emissions. *Nat. Clim. Change* **6**, 42–50 (2016).
4. Doelman, J. C. et al. Afforestation for climate change mitigation: potentials, risks and trade-offs. *Glob. Change Biol.* **26**, 1576–1591 (2020).
5. Food and Agricultural Organisation of the United Nations. *Global Forest Resources Assessments: Terms and Definitions FRA 2020*. (United Nations, 2020); https://www.fao.org/3/I8661EN/i8661en.pdf
6. *Global CO_2 Emissions Rebounded to their Highest Level in History in 2021* (International Energy Agency, 2022).
7. Friedlingstein, P. et al. Global carbon budget 2020. *Earth Syst. Sci. Data* **12**, 3269–3340 (2020).
8. Stavert, A. R. et al. Regional trends and drivers of the global methane budget. *Glob. Change Biol.* **28**, 182–200 (2022).
9. Hansen, J. et al. Young people's burden: requirement of negative CO_2 emissions. *Earth Syst. Dyn.* **8**, 577–616 (2017).
10. Winsten, J., Walker, S., Brown, S. & Grimland, S. Estimating carbon supply curves from afforestation of agricultural land in the Northeastern U.S. *Mitig. Adapt. Strateg. Glob. Change* **16**, 925–942 (2011).
11. Yıldız, O. et al. Restoration success in afforestation sites established at different times in arid lands of Central Anatolia. *Ecol. Manage.* **503**, 378–1127 (2022).
12. Yao, Z., Xiao, J. & Ma, X. The impact of large-scale afforestation on ecological environment in the Gobi region. *Sci. Rep.* **11**, 14383 (2021).

13. *The Role of Desalination in an Increasingly Water-Scarce World* (World Bank, 2019).
14. *The United Nations World Water Development Report 2021: Valuing water*. *Water Politics* (United Nations, 2021).
15. Caldera, U. & Breyer, C. Strengthening the global water supply through a decarbonised global desalination sector and improved irrigation systems. *Energy* **200**, 117507 (2020).
16. Potapov, P. et al. Global maps of cropland extent and change show accelerated cropland expansion in the twenty-first century. *Nat. Food* **3**, 19–28 (2022).
17. Lewis, S. L., Wheeler, C. E., Mitchard, E. T. A. & Koch, A. Regenerate natural forests to store carbon. *Nature* **568**, 3–6 (2019).
18. Bogdanov, D. et al. Low-cost renewable electricity as the key driver of the global energy transition towards sustainability. *Energy* **227**, 120467 (2021).
19. Bogdanov, D., Gulagi, A., Fasihi, M. & Breyer, C. Full energy sector transition towards 100% renewable energy supply: integrating power, heat, transport and industry sectors including desalination. *Appl. Energy* **283**, 116273 (2021).
20. Bastin, J. F. et al. The global tree restoration potential. *Science* **365**, 76–79 (2019).
21. Hofste, R. W. et al. Aqueduct 3.0: updated decision-relevant global water risk indicators. *World Resour. Inst.* https://doi.org/10.46830/WRITN.18.00146 (2019).
22. Arino, O. et al. *Global Land Cover Map for 2009 (GlobCover 2009)* (PANGAEA, 2012); https://doi.org/10.1594/PANGAEA.787668
23. Birge, D., Mandhan, S., Qiu, W. & Berger, A. M. Potential for sustainable use of trees in hot arid regions: a case study of Emirati neighborhoods in Abu Dhabi. *Landsc. Urban Plan.* **190**, 103577 (2019).
24. Pan, Y. et al. A large and persistent carbon sink in the world's forests. *Science* **333**, 988–993 (2011).
25. Pausata, F. S. R. et al. The greening of the Sahara: past changes and future implications. *One Earth* **2**, 235–250 (2020).
26. Kemena, T. P., Matthes, K., Martin, T., Wahl, S. & Oschlies, A. Atmospheric feedbacks in North Africa from an irrigated, afforested Sahara. *Clim. Dyn.* **50**, 4561–4581 (2018).
27. Breyer, C., Fasihi, M., Bajamundi, C. & Creutzig, F. Direct air capture of CO_2: a key technology for ambitious climate change mitigation. *Joule* **3**, 2053–2057 (2019).
28. Luderer, G. et al. Impact of declining renewable energy costs on electrification in low-emission scenarios. *Nat. Energy* **7**, 32–42 (2021).
29. Creutzig, F. et al. The mutual dependence of negative emission technologies and energy systems. *Energy Environ. Sci.* **12**, 1805–1817 (2019).
30. Harper, A. B. et al. Land-use emissions play a critical role in land-based mitigation for Paris climate targets. *Nat. Commun.* **9**, 2938 (2018).
31. Fasihi, M., Efimova, O. & Breyer, C. Techno-economic assessment of CO_2 direct air capture plants. *J. Clean. Prod.* **224**, 957–980 (2019).
32. Mirzabaev, A., Sacande, M., Motlagh, F., Shyrokaya, A. & Martucci, A. Economic efficiency and targeting of the African Great Green Wall. *Nat. Sustain.* https://doi.org/10.1038/s41893-021-00801-8 (2021).
33. Jones, E., Qadir, M., van Vliet, M. T. H., Smakhtin, V. & Kang, S.-M. The state of desalination and brine production: a global outlook. *Sci. Total Environ.* **657**, 1343–1356 (2019).
34. Pistocchi, A. et al. Can seawater desalination be a win-win fix to our water cycle? *Water Res.* **182**, 11596 (2020).
35. Kumar, A., Phillips, K. R., Thiel, G. P., Schröder, U. & Lienhard, J. H. Direct electrosynthesis of sodium hydroxide and hydrochloric acid from brine streams. *Nat. Catal.* **2**, 106–113 (2019).
36. Cruz, C. et al. Using waste brine from desalination plant as a source of industrial water in copper mining industry. *Minerals* **12**, 1162 (2022).
37. Bastin, J. F. et al. Response to comment on 'The global tree restoration potential'. *Science* **364**, 76–79 (2019).
38. Rotenberg, E. & Yakir, D. Contribution of semi-arid forests to the climate system. *Science* **327**, 451–454 (2010).
39. Yosef, G. et al. Large-scale semi-arid afforestation can enhance precipitation and carbon sequestration potential. *Sci. Rep.* **8**, 996 (2018).
40. Rohatyn, S., Rotenberg, E., Tatarinov, F., Carmel, Y. & Yakir, D. Large variations in afforestation-related climate cooling and warming effects across short distances. Preprint at *bioRxiv* https://doi.org/10.1101/2022.09.18.508428 (2022).
41. *Fire, Forests and the Future: A Crisis Raging Out of Control?* (World Wide Fund For Nature, 2020).
42. *Middle East Green Initiative: 'Pathbreaking Work' to Protect the Planet* (United Nations, 2021).
43. Yu, H. et al. The fertilizing role of African dust in the Amazon rainforest: a first multiyear assessment based on data from Cloud-Aerosol Lidar and Infrared Pathfinder Satellite Observations. *Geophys. Res. Lett.* **42**, 1984–1991 (2015).
44. Nogueira, J. et al. Dust arriving in the Amazon basin over the past 7,500 years came from diverse sources. *Commun. Earth Environ.* **2**, 5 (2021).
45. Asiabanpour, B., Ownby, N., Summers, M. & Moghimi, F. Atmospheric water generation and energy consumption: an empirical analysis. *2019 IEEE Texas Power and Energy Conference* https://doi.org/10.1109/TPEC.2019.8662164 (2019).
46. *Scaling Reforestation with Solar-Powered Desalination* (Terraformation, 2020).
47. El Kateb, H. et al. *German-Egyptian Collaboration to Afforestation in Desert Lands of Egypt: Information, Summary and Description of the Field Experiments* (Karl Gayer Institut, 2015).
48. Sarant, L. Egypt: space to grow. *Nature* **544**, S14–S16 (2017).
49. McPherson, E. G., van Doorn, N. & Peper, P. J. *Urban Tree Database and Allometric Equations* General Technical Report PSW-GTR-253 86 (United States Department of Agriculture, 2016); https://doi.org/10.13140/RG.2.2.35769.98405
50. McPherson, E. G., van Doorn, N. S. & Peper, P. J. *Urban Tree Database* (United States Department of Agriculture, 2016).
51. Issa, S., Dahy, B., Ksiksi, T. & Saleous, N. Allometric equations coupled with remotely sensed variables to estimate carbon stocks in date palms. *J. Arid Environ.* **182**, 104264 (2020).
52. Tran, D. B., Hoang, T. V. & Dargusch, P. An assessment of the carbon stocks and sodicity tolerance of disturbed Melaleuca forests in Southern Vietnam. *Carbon Balance Manage.* **10**, 15 (2015).
53. Sohrabi, H., Bakhtiarvand-Bakhtiari, S. & Ahmadi, K. Above- and below-ground biomass and carbon stocks of different tree plantations in central Iran. *J. Arid Land* **8**, 138–145 (2016).
54. Du, H. et al. Carbon storage in a *Eucalyptus* plantation chronosequence in Southern China. *Forests* **6**, 1763–1778 (2015).
55. Stephenson, N. L. et al. Rate of tree carbon accumulation increases continuously with tree size. *Nature* **507**, 90–93 (2014).
56. *FAO Map Catalog - Reference Evapotranspiration (Global - Mean Yearly - ~19km)* (FAO-UN Land and Water Division, 2004).
57. Dhehibi, B. et al. Economic and technical evaluation of different irrigation systems for date palm farming system in the GCC countries: case of Oman. *Environ. Nat. Resour. Res.* **8**, 55 (2018).
58. *Economics of Irrigation Systems* (Texas A & M Univ., 2011).
59. Nisbet, T. *Water Use by Trees* (Forestry Commission, 2005).

60. Manjong, N. B., Oyewo, A. S. & Breyer, C. Setting the pace for a sustainable energy transition in Central Africa: the case of Cameroon. *IEEE Access* **9**, 145435–145458 (2021).
61. Caldera, U. & Breyer, C. The role that battery and water storage play in Saudi Arabia's transition to an integrated 100% renewable energy power system. *J. Energy Storage* **17**, 299–310 (2018).
62. Minx, J. C. et al. Negative emissions - part 1: research landscape and synthesis. *Environ. Res. Lett.* **13**, 063001 (2018).
63. Chen, C. & Tavoni, M. Direct air capture of CO_2 and climate stabilization: a model based assessment. *Clim. Change* **118**, 59–72 (2013).

Acknowledgements

We thank the public financing of Business Finland for the 'P2XENABLE' project (no. 8588/31/2019), the Academy of Finland for the 'Industrial Emissions & CDR' project (no. 329313) and the 'DAC 2.0' project (no. 329313); and LUT University Research Platform 'GreenRenew', which partly funded this research.

Author contributions

U.C. was responsible for the methodology, model development, results analysis, data collection and writing the paper. C.B. was responsible for the methodology, model development, results analysis, reviewing the paper and supervision.

Funding

Open Access funding provided by LUT University (previously Lappeenranta University of Technology (LUT)).

Competing interests

The authors declare no competing interests.

Additional information

Supplementary information The online version contains supplementary material available at https://doi.org/10.1038/s41893-022-01056-7.

Correspondence and requests for materials should be addressed to Upeksha Caldera or Christian Breyer.

Peer review information *Nature Sustainability* thanks Hilarydoss Sharon, Eliodoro Chiavazzo and the other, anonymous, reviewer(s) for their contribution to the peer review of this work.